HRTS OBSERVATIONS OF THE FINE STRUCTURE AND DYNAMICS OF THE SOLAR CHROMOSPHERE AND TRANSITION ZONE

Kenneth P. Dere
E. O. Hulburt Center for Space Research
Naval Research Laboratory
Washington, D.C. 20375

ABSTRACT

Arc-second UV observations of the Sun by the NRL High Resolution Telescope and Spectrograph (HRTS) have led to the discovery of dynamic fine structures such as 400 km s^{-1} coronal jets and chromospheric jets (spicules) and have provided new information about the structure and dynamics of the transition zone. These observations are reviewed and their relevance to the origin of the solar wind is discussed.

Introduction

Recent results derived from UV observations of the solar chromosphere and transition zone made by the NRL High Resolution Telescope and Spectrograph (HRTS) are presented here. These observations have an inherent interest since they are made with the highest spatial resolution yet obtained in the UV and show the first UV observations of solar fine structure. They are also of specific interest to this conference since the solar wind and many of its disturbances presumably originate somewhere near the solar surface. The HRTS instrument consists of a Cassegrain telescope which focuses a solar image with 1 arc-sec. resolution onto the slit jaw of the spectrograph which produces stigmatic photographic spectra of the 1000 arc-sec. long slit in the 1175-1710 Å wavelength range. To date, there have been four rocket flights of the HRTS instrument (referred to as HRTS 1-4) and it is scheduled to be flown on Spacelab 2.

The Chromosphere

Figure 1 shows some of the general properties of the quiet Sun in the HRTS spectra. On the left is a spectroheliogram obtained in Hα by Sacramento Peak Observatory essentially simultaneously with the HRTS spectra obtained during the third flight. The Hα image consists of dark absorption features, the dark mottles, which outline the supergranulation cells. Also indicated is the position of the HRTS slit and the corresponding stigmatic spectra in lines of C I (10^4 K), Si II (2×10^4 K) and C IV (10^5 K). All three ions show intense emission where the slit crosses the supergranular cell boundaries although the C IV emission appears in some cases to be shifted towards the limb. This is consistent with limb brightening curves which show C IV to be produced 4 arc-sec. above the photosphere. An absolute wavelength scale can be determined from the narrow Si I lines in the vicinity with a accuracy of about 2 km s^{-1}.

Examples of small scale structures observed in the HRTS spectra are shown in Figure 2. Here, a short segment of HRTS 1 C IV and C I spectra near the limb are displayed. At the top of the C IV spectra is a coronal jet with line

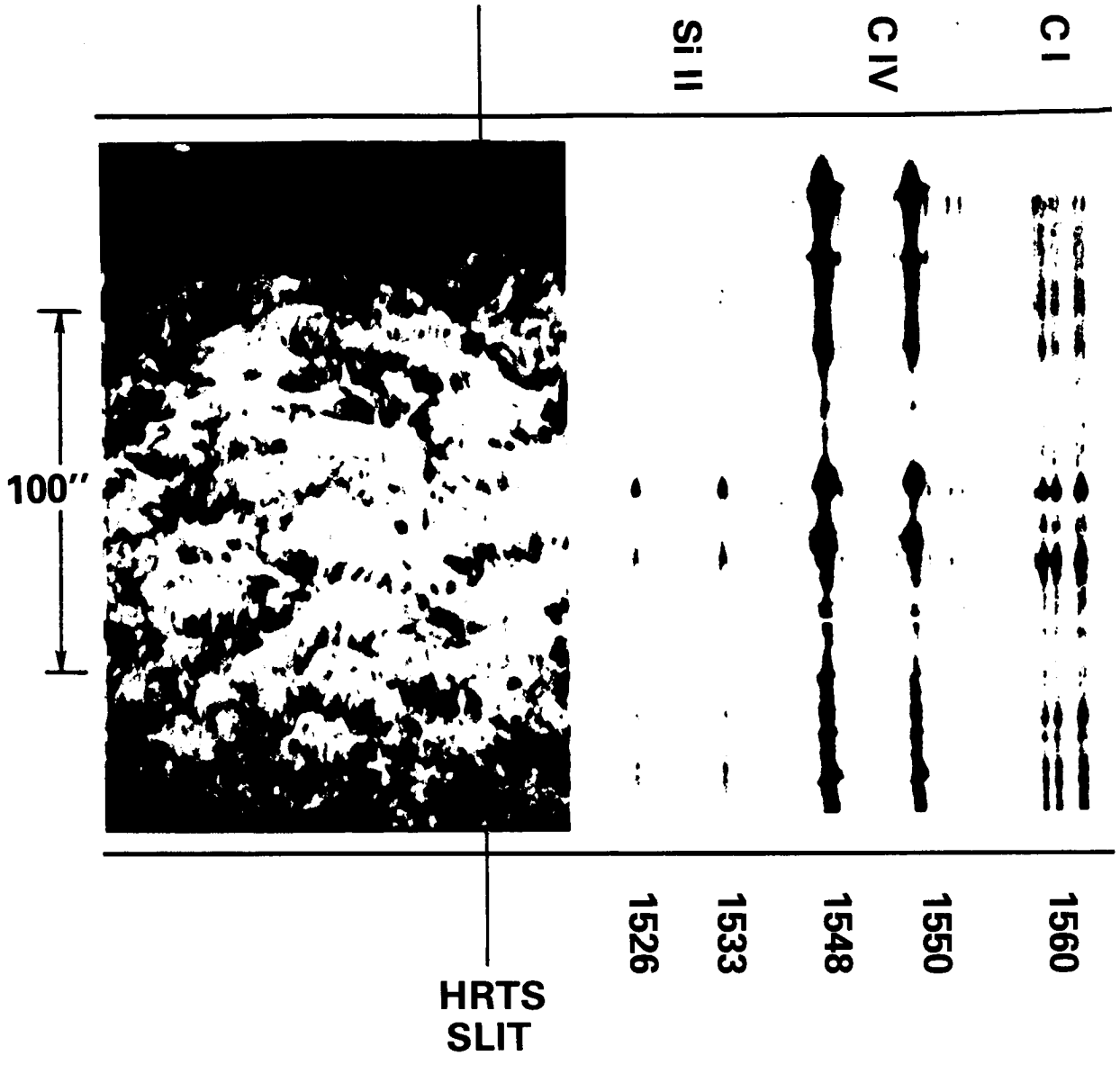

Figure 1. HRTS spectra of Si II, C IV, C I and an Hα spectroheliogram at the limb of the solar south pole.

of sight velocities of 200 km s^{-1} and projected radial velocities of 400 km s^{-1}. Shifts to the left are blueshifts and are caused by plasma moving toward the observer or away from the Sun. Near the bottom of that figure is a "turbulent" event characterized by wide, symmetric C IV profiles which are produced by random nonthermal velocities on the order of 150 km s^{-1}. In the C I spectra, at least six chromospheric jets are seen as emission features in the line wings which are caused by plasma moving at 10-20 km s^{-1}. It is interesting to note that the coronal jet and turbulent event seen in C IV have no noticeable cospatial signature in the C I profiles and the chromospheric jets seen in C I both occur where the C IV intensity is quite low. This is true for the particular events seen in Figure 2 and in general.

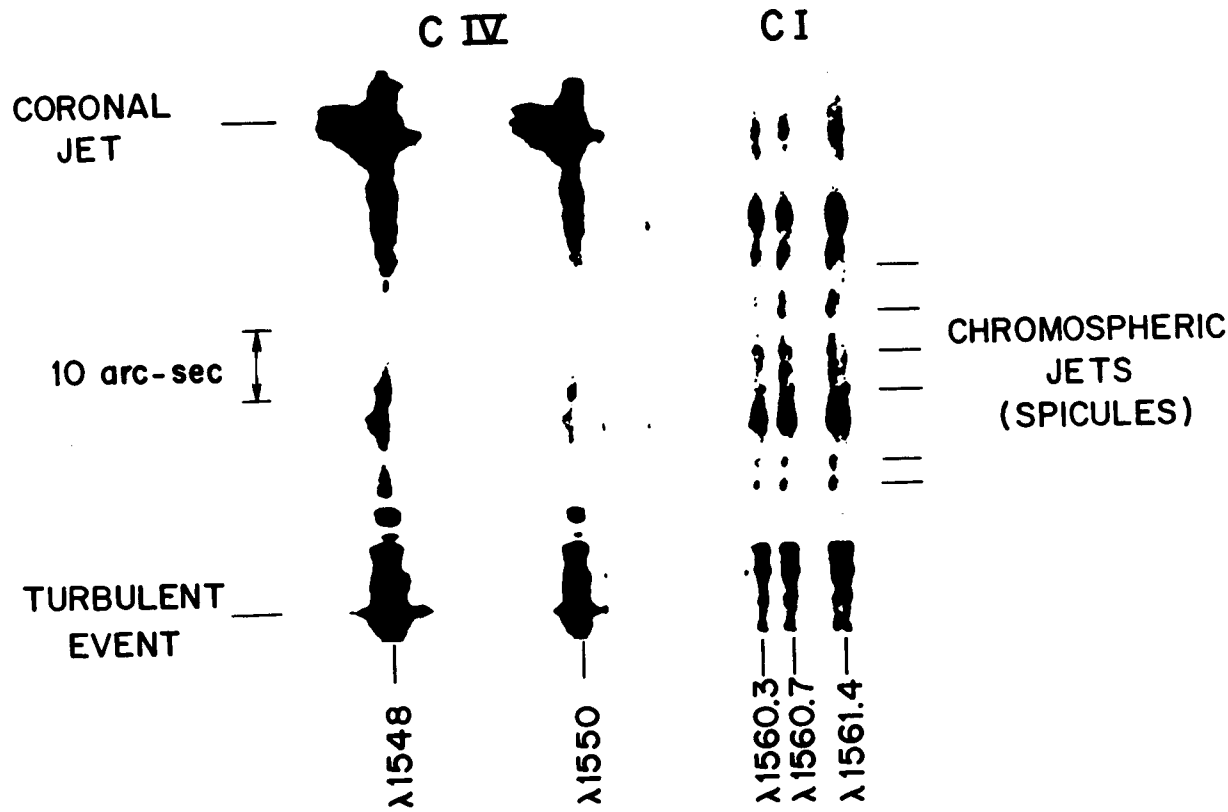

Figure 2. Examples of fine structures observed in HRTS spectra: coronal jets, turbulent events and chromospheric jets (spicules).

Spicules, which play a important role in the convective transport in the solar atmosphere, have been seen in visible light above the solar limb for over a hundred years. They are slender jets of gas which are observed to rise and often fall at a velocity of 25 km s^{-1}. However, there has never been an identification of spicules with any known phenomenon on the disk although it is often assumed that they are the dark Hα mottles. We now believe there is sufficient evidence to identify the chromospheric jets seen in Figure 2 as spicules on the disk (Dere, Bartoe and Brueckner, 1983).

Typically the chromospheric jets (spicules) have a size of 1-2 arc-sec. projected along the slit and twice as many blue shifted (rising) events are seen as the weaker redshifted (falling) events. It is possible that with greater sensitivity we would see equal numbers of the two. The chromospheric jets can be seen in other lines of C I such as the allowed multiplet at 1657 Å and the intercombination lines near 1613 Å as well as in lines of other chromospheric ions such as Si I, Si II and S I. However, they are not seen in lines of somewhat hotter ions such as C II or Si III and as we have previously noted, C IV is often extremely weak at the sites of chromospheric jets. Clearly they are exclusively a chromospheric phenomenon. Spicule profiles of the C I 1560 Å lines are shown in Figure 3 as well as nearby nonspicular profiles for comparison. The spicular emission peak is shifted to the blue by .05 to .1 Å

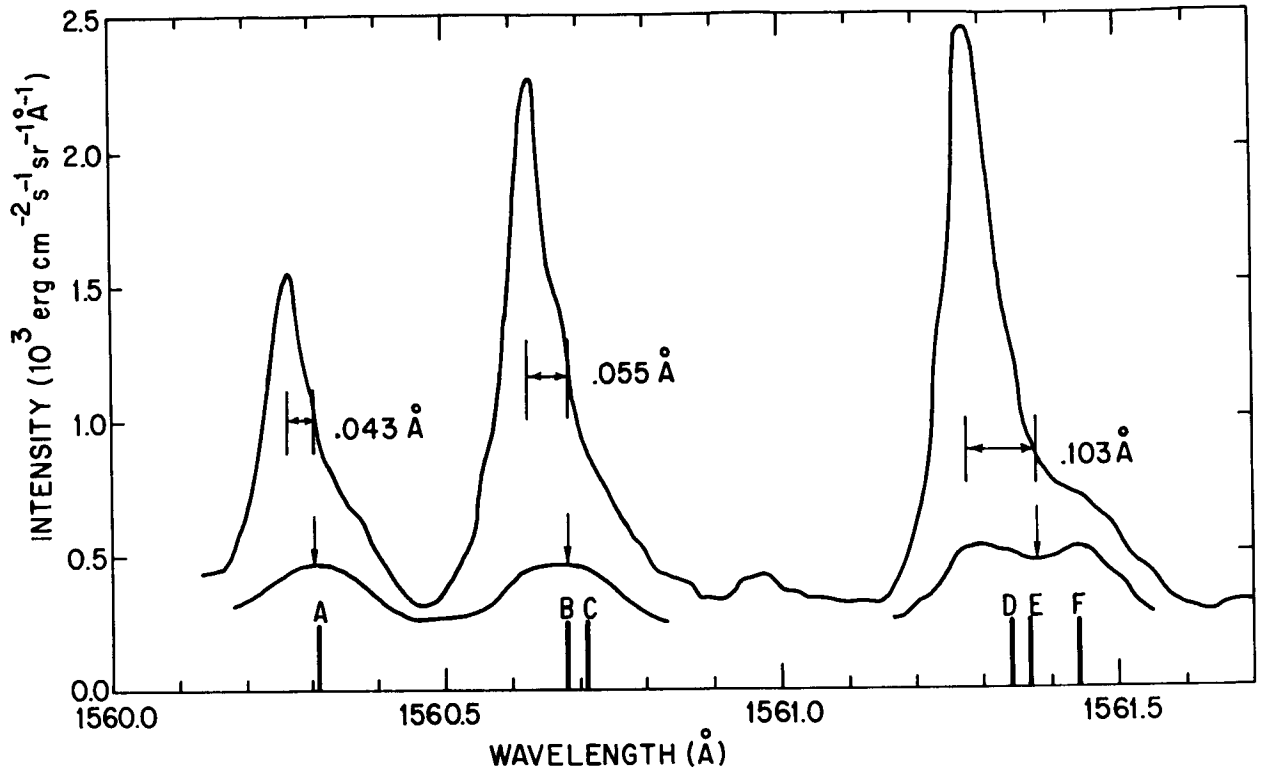

Figure 3. The profiles of the C I lines near 1560 Å in a spicule. The arrows indicate the observed average wavelength of the three lines (blends) made up of the five C I lines labelled A through F.

corresponding to line of sight velocities of 10 to 20 km s^{-1} and shows no self reversal as do more typical nonspicular profiles. From the intensity and lack of self absorption in these profiles a temperature of 1.6 x 10^4 K and density of 10^{11} cm^{-3} are derived. These are comparable to what is found from visible light observations.

Many observers have come to believe that the dark Hα mottles observed on the disk should be identified with the spicules seen at the limb although a study of Hα mottle profiles (Grossmann Doerth and v. Uexkull, 1971) shows that the velocities in the mottles are significantly lower than those in spicules. This same study did find region of 20 km s^{-1} flows but only in "quite unconspicuous, little gray features" which were not considered important. Our own observations confirm the low velocities in the supergranular cell boundaries where the mottles are found. The chromospheric jets (spicules), while not as bright as the network emission, are nevertheless quite conspicuous in the ultraviolet spectra. The chromospheric jets are generally unrelated to the dark Hα mottles.

In conclusion, we confirm many of the known physical properties of spicules derived from ground-based observations as is to be expected. The surprising new result is that spicules occur in the supergranulation cell interiors and not at the boundaries where the strongest magnetic fields tend to be clustered.

The Transition Zone

The two strong C IV lines near 1550 Å are our primary diagnostics for the transition zone. Both lines are formed around 10^5 K and are optically thin on the disk. The regions viewed by the HRTS 3 slit include the limb above a polar coronal hole which extended up to a latitude of 50°, mostly quiet Sun and a filament near Sun center. We quantify the information in the profiles by taking moments of the wavelength weighted by the specific intensity. In this way we derive the integrated line intensity, the net Doppler velocity and the line width. These three quantities are shown in Figure 4 for HRTS 3 data along the entire slit. Some of the more intense regions, such as the limb, are over-

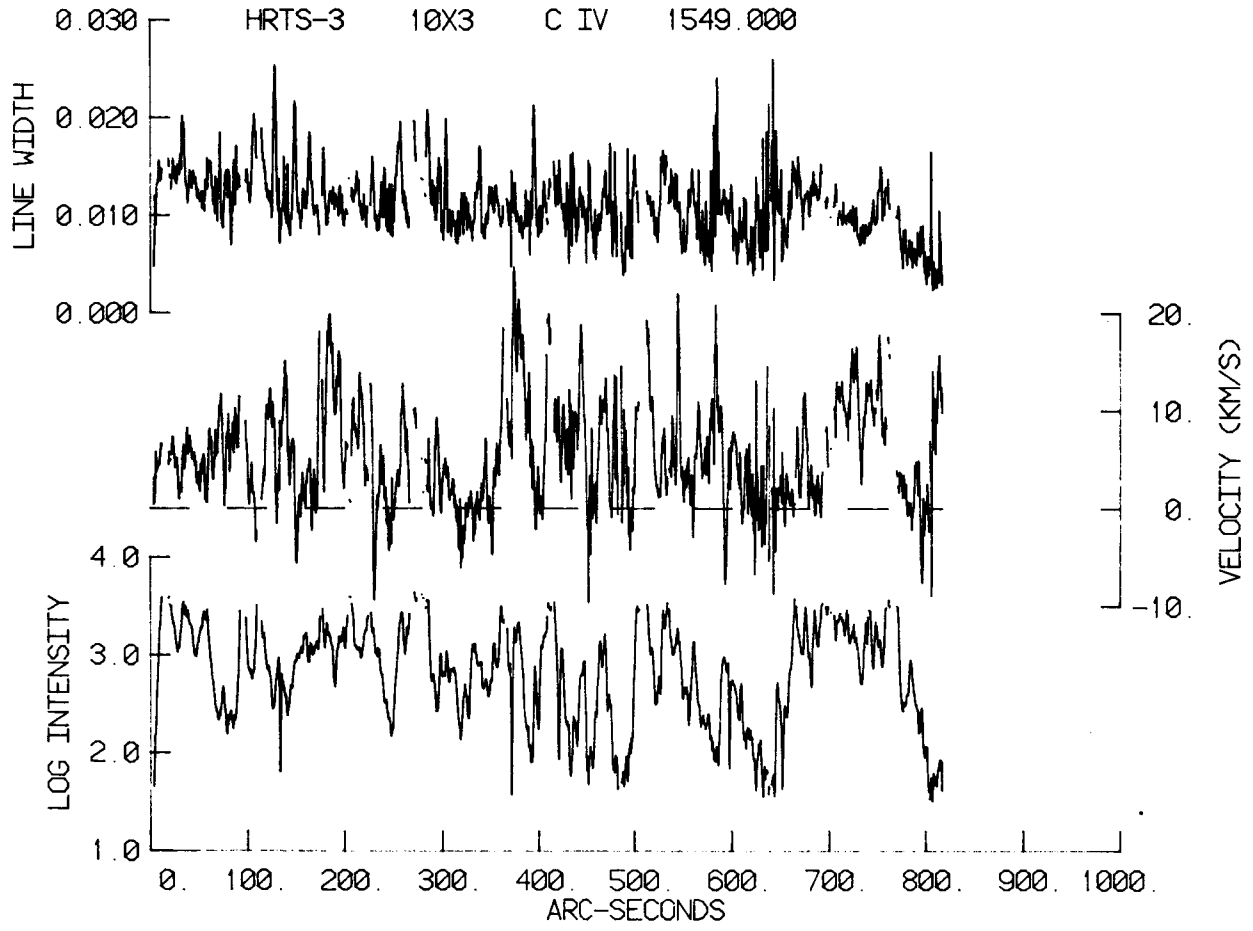

Figure 4. Intensity (erg cm^{-2} s^{-1} sr^{-1}), velocity (km s^{-1}) and line width ($Å^2$) for C IV λ1548 and λ1550 as a function of position along the slit.

exposed and are not plotted. The limb defined by the continuum is near an indicated height of 17 arc-sec. Again, the regions of high C IV intensity generally pick out the chromospheric network although there is no strong point for point correlation with C I intensities which also pick out the network. In fact, from their respective autocorrelation coefficients for line intensity, the C IV transition zone structures have a typical size of 1.5 arc-sec compared

to 8 arc-sec for the C I chromospheric structures. Preliminary two-dimensional images in C I and C IV show this large scale relationship (the network) between the two but show little similarity in the small scale features.

The line of sight velocities displayed in Figure 4 are predominately away from the observer and from this one can conclude that the transition zone consists of material generally falling toward the solar surface. The velocity data, as summarized in Figure 5, do show some regions of upflows but the average Doppler shift is 0.028 Å which corresponds to a downflow a 5.4 km s^{-1}

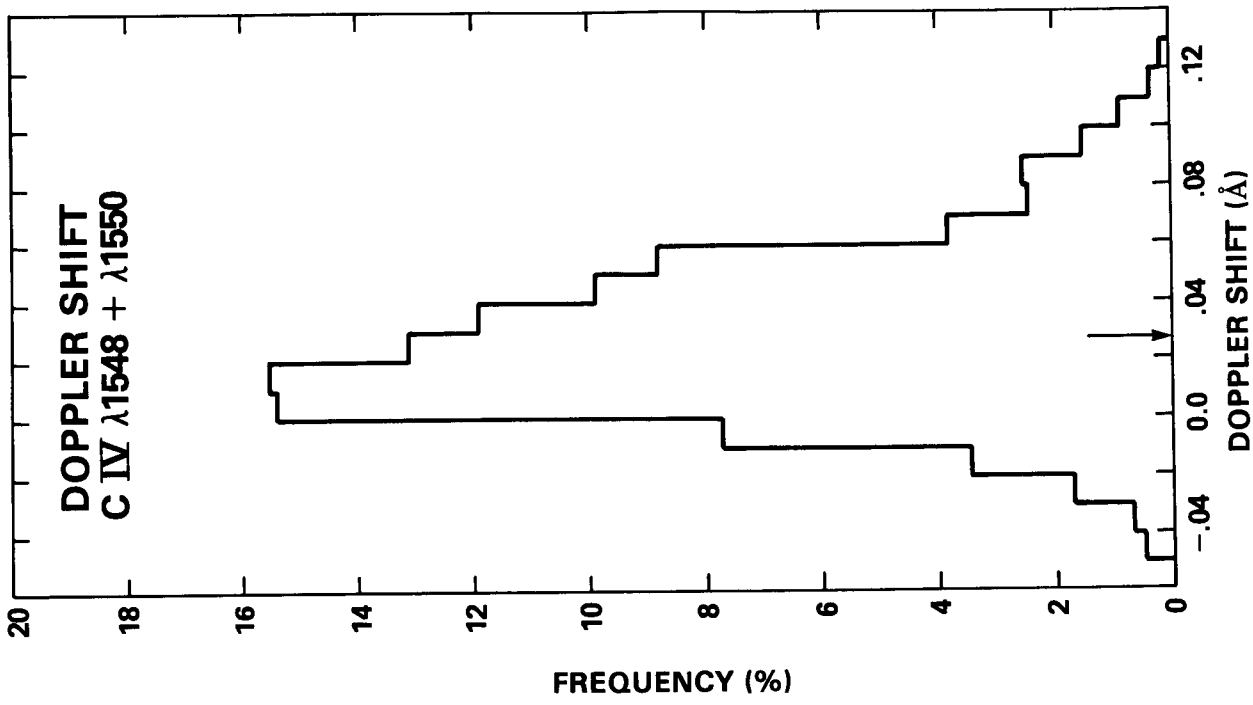

Figure 5. Relative frequency of occurrence of the C IV Doppler shifts.

at disk center. We emphasize that our velocity scale is relative to the narrow chromospheric Si I lines and should be accurate to 0.01 Å or 2 km s^{-1}. Above the limb redshifts are also seen. An examination of these C IV line profiles shows that their peak is near the rest wavelength and the derived redshift is due to the greater strength of the red wing as compared with the blue. As we noted, a polar hole extended up to a latitude of about 50° during the HRTS 3 flight. This latitude corresponds to a relative position of 240 arc-sec on Figure 4. There is no sign of major large scale outflows in the transition zone of this polar coronal hole. Using a wavelength scale referenced to chromospheric lines, Doschek, Feldman and Bohlin (1976) also find little evidence for outflows in coronal holes. Rottman and Orrall (1982) show a relative blueshift between coronal holes and other solar regions but in the light of the above results, it is not clear that this can be interpreted as an absolute blueshift in coronal holes.

Previous studies of the transition zone at lower resolution (Lites et al. 1976 and Gebbie et al. 1981) have found that regions of downflow are correlated with regions of high intensity. However our own data show no real correlation between these two quantities as presented in Figure 6. In a large

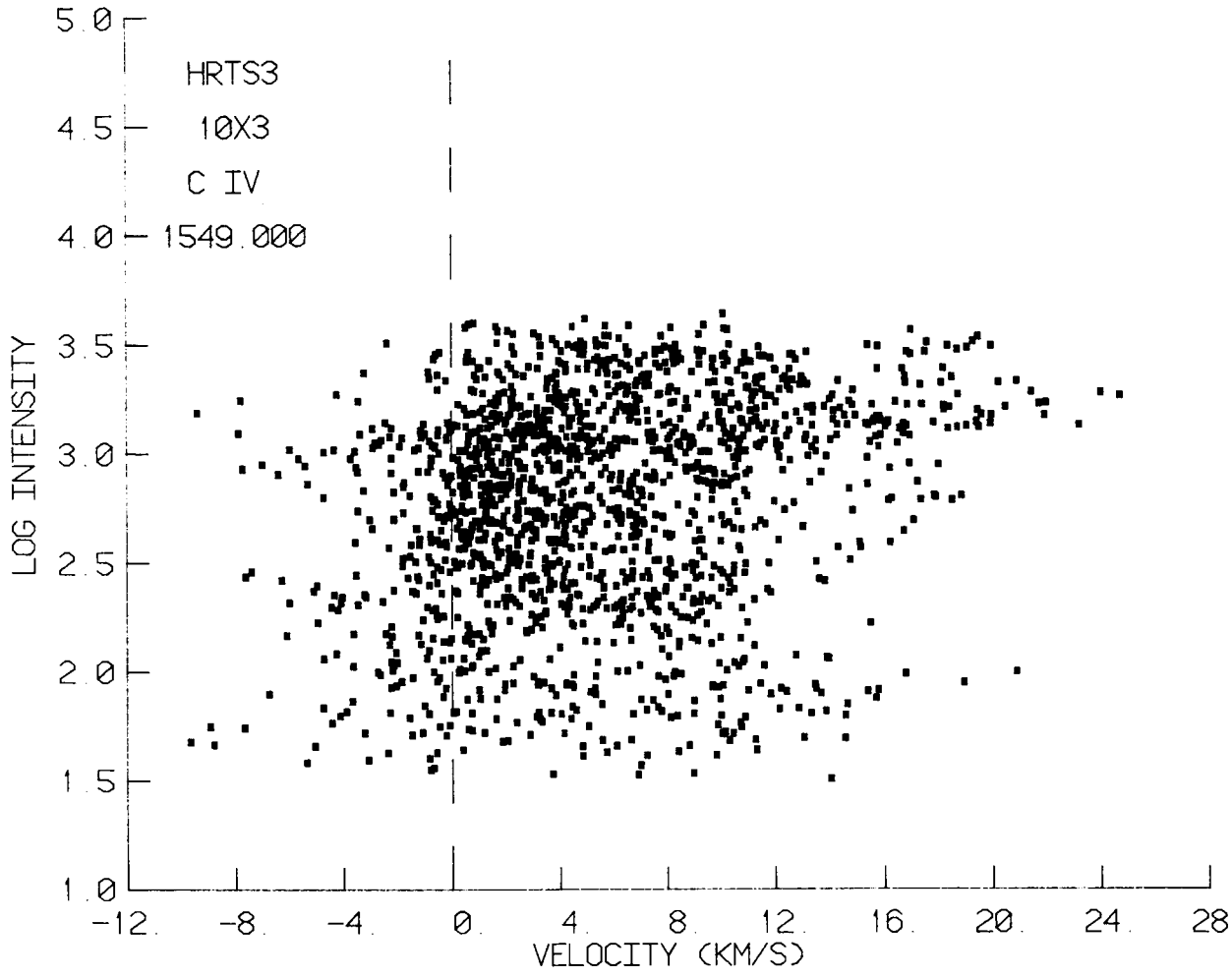

Figure 6. A scattergram of C IV intensity versus C IV velocity near Sun center.

scale sense, there are certainly some bright regions which show strong downflows but this relationship breaks down in general and when these regions are examined in detail. An autocorrelation analysis also shows that the size of the bright C IV regions is around 1.5 arc-sec. and the 3 arc-sec. size of the flowing structures is significantly larger.

The line width data shown in Figure 4 reveal a number of wide profile events along the slit which consist of both the jets and the turbulent events, examples of which were displayed in Figure 2. Brueckner and Bartoe (1983) provide a detailed anlysis of the jets and turbulent events. Even the more typical profiles have a line width which requires turbulent or nonthermal

velocities on the order of 21 km s^{-1} together with thermal broadening to explain the observed width. The rise in the line width toward the limb is due to the integration over an increasingly larger number of flow fields.

Turbulent velocities in the turbulent events range from 50 km s^{-1} to 250 km s^{-1}. Most of these events occur only once but some of the larger ones are observed to reoccur at the same position in our 4 minute observing time. Size scales are often at the instrumental resolution (1 arc-sec.). They are seen in lines spanning the temperature range 2 x 10^4 to 2 x 10^5 K although apparently similar events have also been observed in coronal (2 x 10^6 K) lines in the Skylab data.

A time history of one of the more spectacular jets is shown in Figure 7.

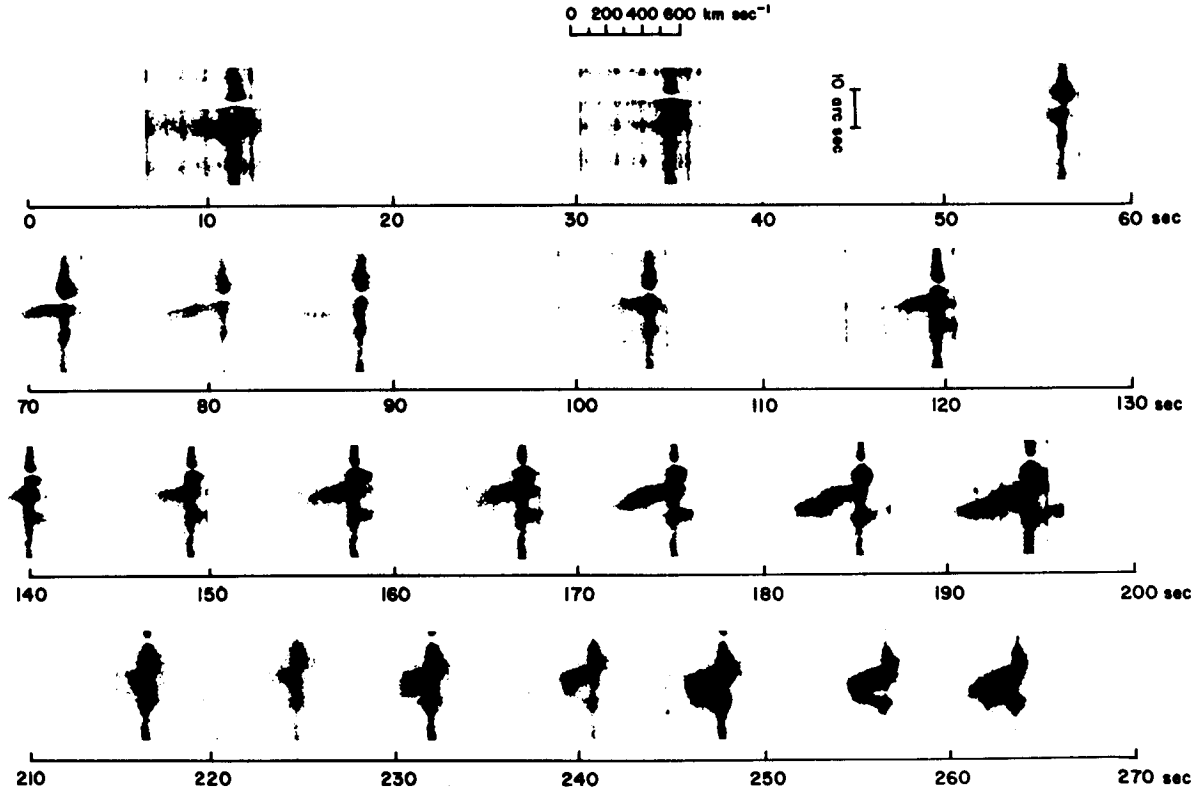

Figure 7. A time sequence of coronal jets observed in C IV.

This particular jet, seen as the strongly blue shifted emission in C IV λ1548, appears four times at the same location during a four minute rocket flight. The maximum velocities which reach 400 km s^{-1} are consistent with an acceleration of 5 km s^{-2} that persists throughout the observed lifetime. The jets contain material over a wide range of temperatures (2 x 10^4 - 2 x 10^5 K). One interpretation is that of a magnetic loop being expelled outward through the solar atmosphere. The Hα slit jaw pictures do not show any feature that might correspond to the jets.

The time sequence of C IV spectra in Figure 8 shows numerous examples of a less spectacular but more prevalent sort of jet. These have maximum velocities of from 80 to 150 km s^{-1} and often have both blueshifted and redshifted components. Their size is generally near the instrumental resolution.

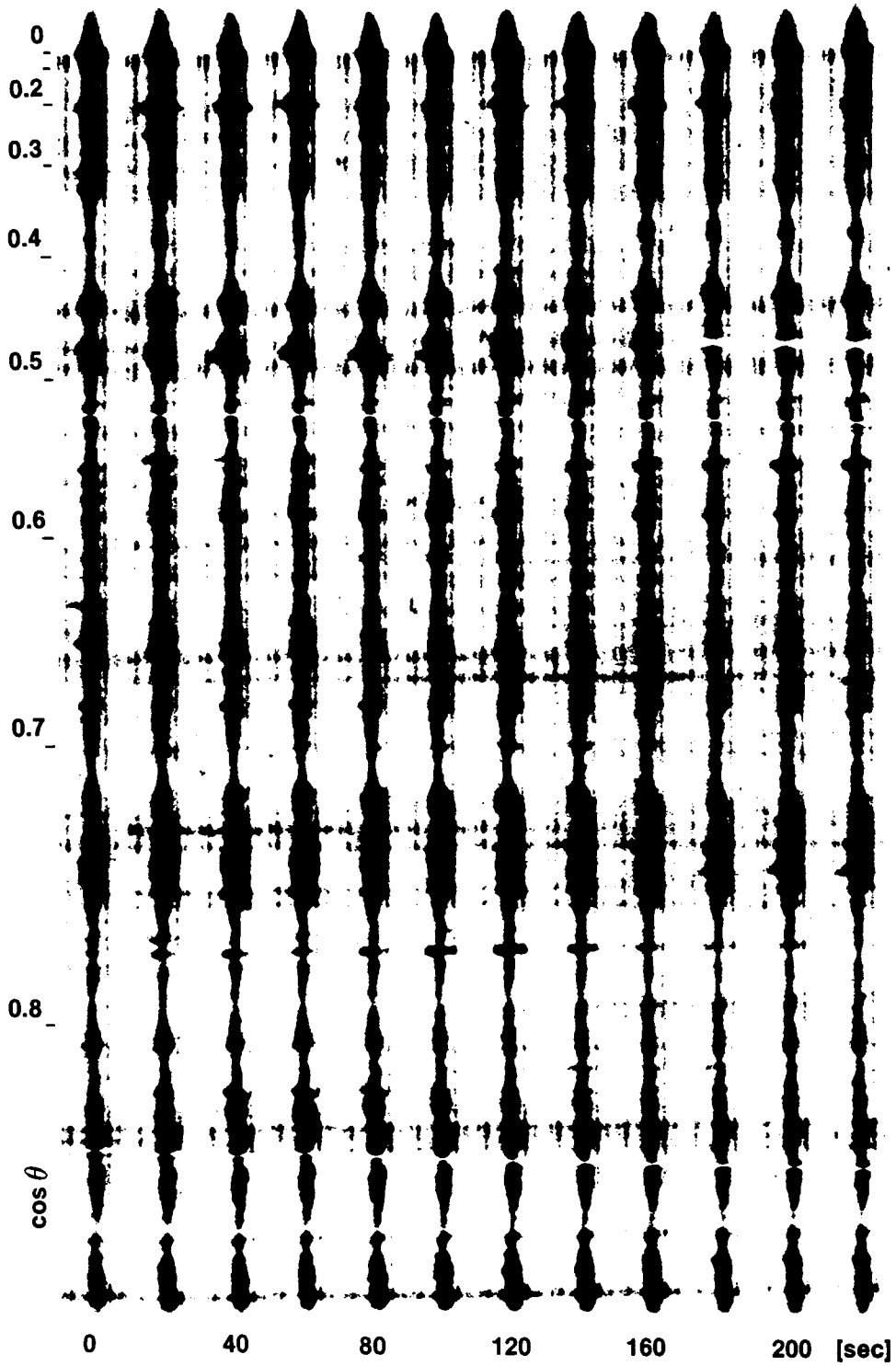

Figure 8. A time sequence of C IV spectra showing numerous 100 km s^{-1} jets.

Origin Of The Solar Wind

The solar wind has an associated mass flux of 2×10^{12} g s^{-1} which must be present at chromospheric and transition zone levels and should be observable with suitable instrumentation. In the chromosphere the only significant vertical flows that we observe are in the spicules; about 2/3 are outflows and 1/3 downflows (since the downflows are less intense, it is possible that there are equal numbers of each). Roughly only one in 10 spicules produces a measurable blueshift in the transition zone. From a density of 10^{10} cm^{-3}, a velocity of 25 km s^{-1} and a fill factor of 2%, the average outward mass loss in spicules observed at transition zone temperatures is 2×10^{13} g s^{-1}, an order of magnitude above solar wind requirements. The downward mass flow in the transition zone for a pressure $n_e T_e = 10^{15} cm^{-3}$ K and a velocity of 5 km s^{-1} is 5×10^{14} g s^{-1}. This latter figure assumes a fill factor of unity which rests on the interpretation of the transition zone as an extremely thin (20 km) layer. Since most high resolution spectroheliograms of the upper chromosphere and corona show the ubiquitous presence of filamentary structures, it is likely that the transition zone has a similar consistency. In that case, fill factors of 0.1 can be derived and the downward transition zone mass flow is reduced to 5×10^{13} g s^{-1} still an order of magnitude above the solar wind value.

The are two ways to consider these order of magnitude mass flow estimates. First, the origin of the solar wind can be explained with only small changes in these very rough numbers, so that the transition zone downflows return the spicular mass not needed to sustain the solar wind. The second approach is to say that the spicule upflows and transition region downflows constitute a closed circulation system with no mass flux available for the solar wind. It is perhaps even more likely that the spicules themselves produce no net mass transport. In this case we must look elsewhere. The HRTS data suggest the jets as likely candidates (Brueckner, Bartoe and VanHoosier, 1977).

An upper limit on the mass in one of the numerous 100 km s^{-1} jets is about 3×10^{8} g. The birthrate for these jets is 170 s^{-1} on the solar surface and the consequent mass loss is about 5×10^{10} g s^{-1} which is much less than that in the solar wind. The mass content in the large 400 km s^{-1} jet seen in Figure 8 is estimated to be 2×10^{11} g. During three rocket flights, a total of six large jets have been observed. In the third flight which had the greatest spatial coverage, only one of the large jets was observed and a rate of 4 jets per second on the entire solar surface was derived. Observations of jet-like structures in C IV spectroheliograms above the limb indicate that on the entire solar surface, jets occur at the rate of 5 s^{-1}. Thus the mass loss due to the large 400 km s^{-1} jets is 10^{12} g s^{-1}, which is quite close to the mass loss of the solar wind. The kinetic energy released in these jets is 3×10^{28} erg s^{-1} which is higher than the total energy flux in the solar wind at the Sun. Thus, there is sufficient mass and energy in these high speed jets to supply the solar wind. Such a non-steady source would imply highly variable solar wind parameters, especially near the Sun.

References

Brueckner, G. E., A High Resolution View of the Solar Chromosphere and Corona, Highlights of Astronomy, 5, 557 1980.

Brueckner, G. E. and J.-D. F. Bartoe, Observations of High Energy Jets in the Corona and the Acceleration of the Solar Wind, Ap. J., in press, 1983.
Brueckner, G. E., J.-D. F. Bartoe and M. E. VanHoosier, High Spatial Resolution Observations of the Solar EUV Spectrum, Proc. of the OSO-8 Workshop, 1977.
Dere, K. P., J.-D. F. Bartoe and G. E. Brueckner, Chromospheric Jets: Possible EUV Observations of Spicules, Ap. J. (Letters), in press, 1983.
Doschek, G.A., U. Feldman and J. D. Bohlin, Doppler Wavelength Shifts of Transition Zone Lines Measured in Skylab Solar Spectra, Ap. J. (Letters), 205, L177, 1976.
Gebbie, K. B. et al., Steady Flows in the Solar Transition Region Observed with SMM, Ap. J. (Letters), 251, L115, 1981.
Grossmann-Doerth, U. and M. v. Uexkull, Spectral Investigations of Chromospheric Fine Structure, Solar Phys., 20, 31, 1971.
Lites, B. W., E. C. Bruner, E. G., Chipman, G. A. Shine, G. J. Rottman, O. R. White, and R. G. Athay, Preliminary Results from the Orbiting Solar Observatory 8: Persistent Velocity Fields in the Chromosphere and Transition Region, Ap. J. (Letters), 210, L11, 1976.
Rottman, G. J. and F. Q. Orrall, Observational Evidence for Solar Wind Acceleration at the Base of Coronal Holes, This conference, 1982.